$B^0_{(s)} \to \pi^0\pi^0, \eta\eta$ measurement and CKM angle α (ϕ_2) determination using $B \to \pi\pi$ at CEPC

Yuexin Wang, Lingfeng Li, Shanzhen Chen , Manqi Ruan

Joint Workshop of the CEPC Physics, Software and New Detector Concept
May 23-25, 2022

Status of $B^0_{(s)} \to \pi^0\pi^0, \eta\eta$

Experimental and theoretical branching ratios (in units of 10^{-6})

Channel	DATA	SCET [1]	QCDF	pQCD
$B^0 \to \pi^0\pi^0$	1.59 ± 0.26 [2]	$0.84 \pm 0.29 \pm 0.30 \pm 0.19$	$0.30^{+0.46}_{-0.26}$	$0.24^{+0.09}_{-0.07}$
$B^0_s \to \pi^0\pi^0$	< 210 [3]	-	$0.13^{+0.05}_{-0.05}$ [10]	$0.21^{+0.10}_{-0.09}$ [5] $0.28^{+0.08+0.04+0.01}_{-0.07-0.05-0.00}$ [4]
$B^0 \to \eta\eta$	< 1 [6]	$0.69 \pm 0.38 \pm 0.13 \pm 0.58$ $1.0 \pm 0.4 \pm 0.3 \pm 1.4$	$0.32^{+0.13+0.07}_{-0.05-0.06}$ [7] $0.16^{+0.03+0.43+0.09+0.10}_{-0.03-0.18-0.03-0.05}$ [8]	0.067 [9]
$B^0_s \to \eta\eta$	< 1500 [3]	$7.1 \pm 6.4 \pm 0.2 \pm 0.8$ $6.4 \pm 6.3 \pm 0.1 \pm 0.7$	$10.9^{+6.3+5.7}_{-4.0-4.2}$ [10]	$10.4^{+4.9}_{-3.4}$ [5]

- Only $B^0 \to \pi^0\pi^0$ has been observed experimentally
  - $B^0 \to \pi^0\pi^0$
    - Puzzle: discrepancy between experimental and theoretical BR
    - Necessary to determine CKM angle alpha
  - Charmless two-body hadronic B-meson decay
    - experimentally clean
    - hadron physics, even new physics

Advantage of CEPC

- Tera-Z factory
  - Massive b-hadrons
    ~10^{11} B^0 & ~10^{10} B_s^0
  - Larger boost of b-hadrons than Belle II → more precise vertex reconstruction
- Lepton collider
  - Cleaner collision environment and much lower background level
  - Benefit neutral final states reconstruction

b-hadrons	Belle II	LHCb (300 fb^{-1})	Tera-Z
B^0, $\bar{B}^0$	5.4×10^{10} (50 ab^{-1} on $\Upsilon(4S)$)	3×10^{13}	1.2×10^{11}
$B^{\pm}$	5.7×10^{10} (50 ab^{-1} on $\Upsilon(4S)$)	3×10^{13}	1.2×10^{11}
B_s^0, $\bar{B}_s^0$	6.0×10^{8} (5 ab^{-1} on $\Upsilon(5S)$)	1×10^{13}	3.1×10^{10}
$B_c^{\pm}$	-	1×10^{11}	1.8×10^{8}
Λ_b^0, $\bar{\Lambda}_b^0$	-	2×10^{13}	2.5×10^{10}

Key detector performance

- Fast simulation strategy
- b-jet tagging
  - CEPC baseline: $\varepsilon \sim 80\%,\ p \sim 90\%$
- ECAL performance
  - Only focus on di-photon decay of π^0 and η
  - B mass resolution: $\sigma_{m_B} \sim 30\text{MeV} \rightarrow 2\sigma$ separation between B^0 and B_s^0
  - EM resolution: $3\%/\sqrt{E} \oplus 0.3\%$

CEPC baseline b-tagging

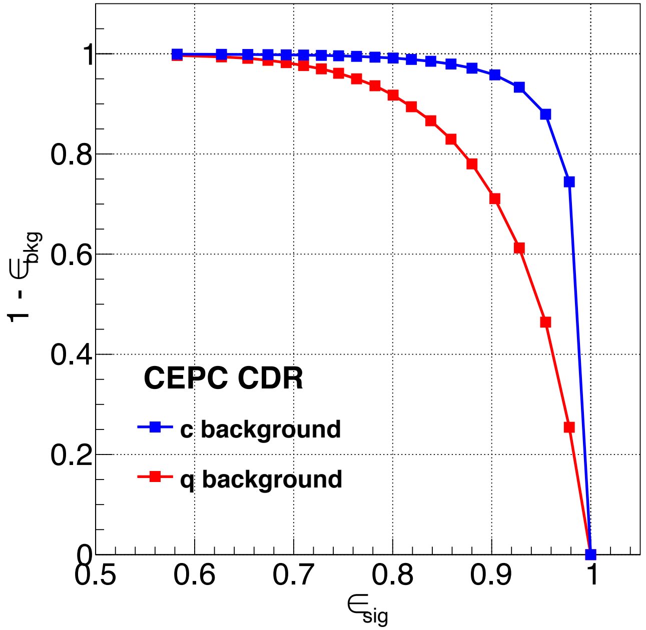

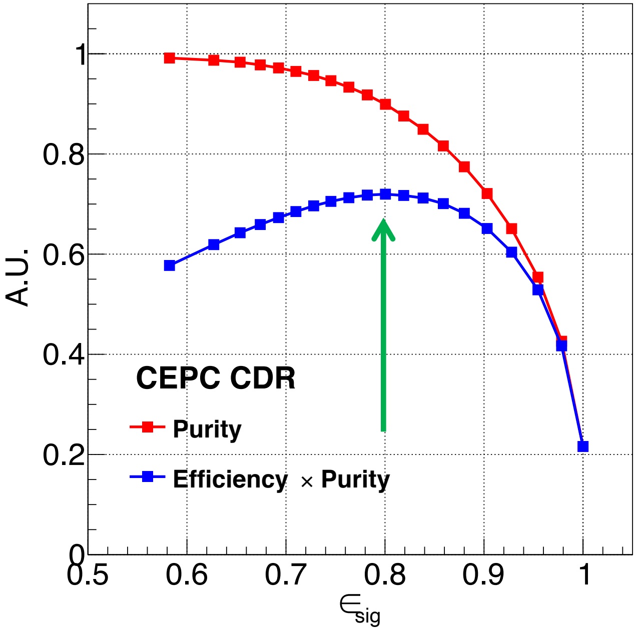

B^0 B_s^0 separation

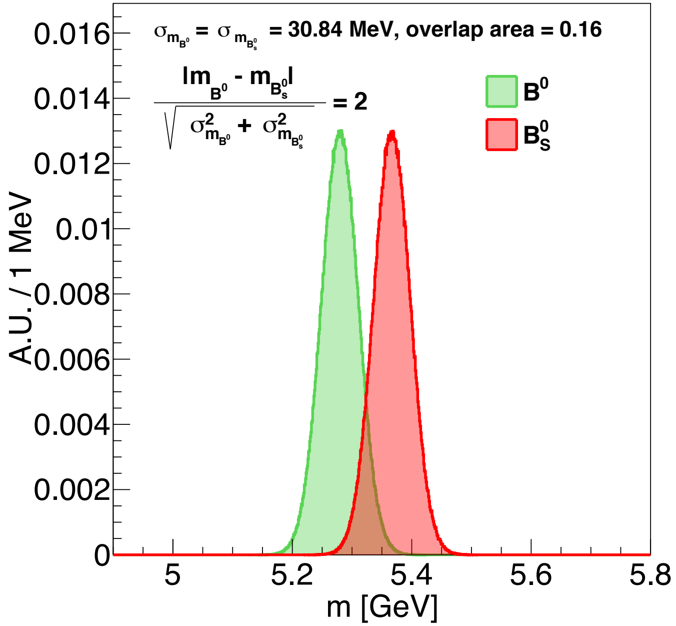

Reconstruction performance of π^0 and η

- Inclusive π^0 and η in $Z \to q\bar{q}$ (91.2 GeV)
  - $\bar{N}_{\pi^0} \gg \bar{N}_{\eta}$
  - prioritize π^0 reconstruction, use remaining γ to reconstruct η
- Optimal $\epsilon \times p$ vs $E_{\pi^0,\eta}$
  - $> 90\%$ for $E_{\pi^0} > 10$ GeV
  - $> 60\%$ for $E_{\eta} > 10$ GeV

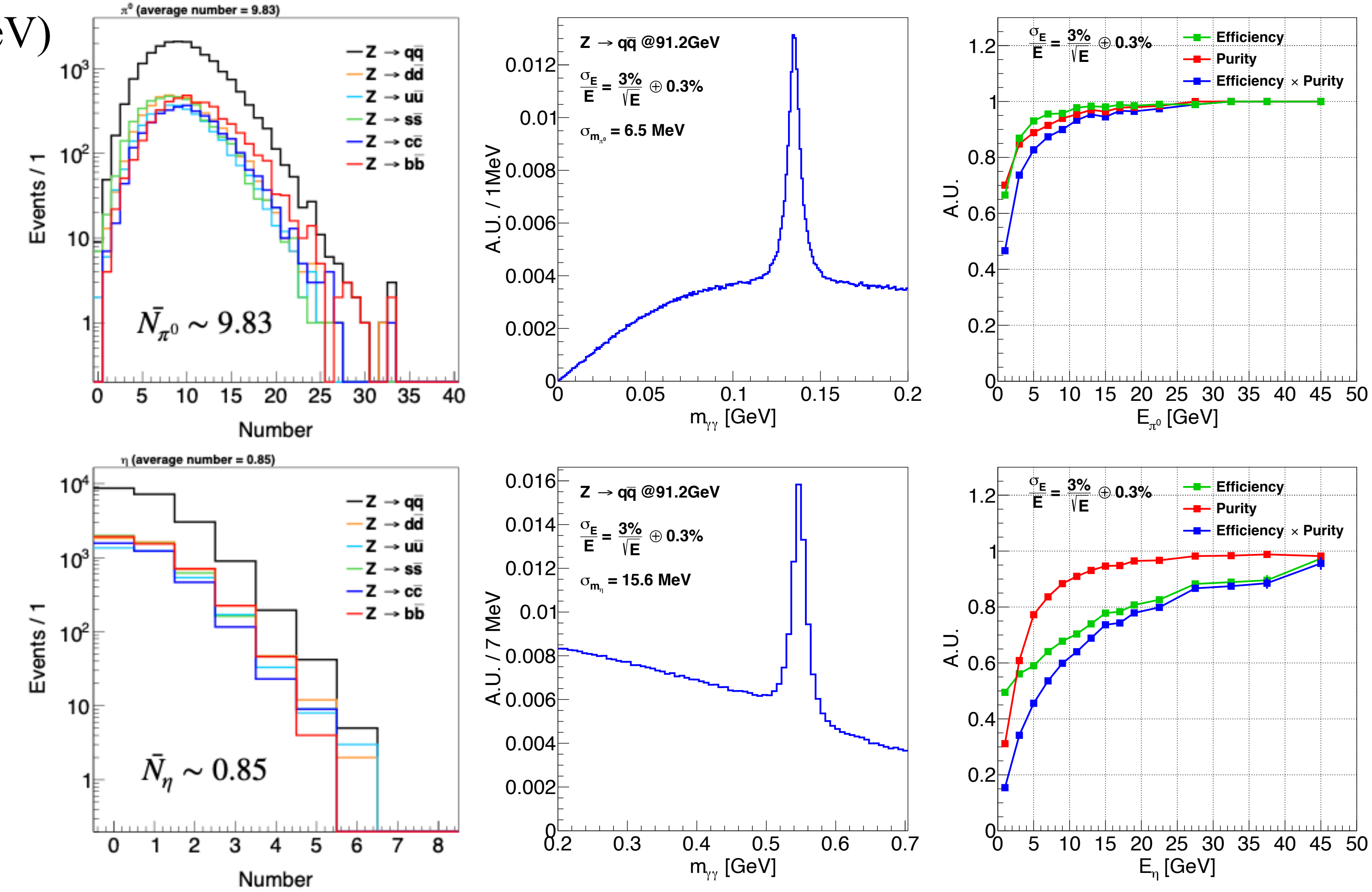

Event selection of $B^0_{(s)} \to \pi^0\pi^0$

Selection chain	$B^0 \to \pi^0\pi^0 \to 4\gamma$	$B^0_s \to \pi^0\pi^0 \to 4\gamma$	$u\bar{u}+d\bar{d}+s\bar{s}$	$c\bar{c}$	$b\bar{b}$	$\sqrt{S+B}/S$
Yield at Tera-Z	191113	8948	4.29×10^{11} (61.21%)	1.20×10^{11} (17.19%)	1.51×10^{11} (21.60%)	
b-tagging	152890	7159	3.64×10^{9} (2.70%)	9.94×10^{9} (7.38%)	1.21×10^{11} (89.92%)	
$\pi^0 \to \gamma\gamma$	148213	6953	3.61×10^{9}	9.91×10^{9}	1.21×10^{11}	
Lower $E_{\pi^0} > 6$ GeV	92407	4391	8.44×10^{8}	1.60×10^{9}	1.31×10^{10}	
Higher $E_{\pi^0} > 14$ GeV	87355	4142	3.08×10^{8}	3.15×10^{8}	1.91×10^{9}	
$E_{\pi^0\pi^0} > 22$ GeV	87073	4127	2.90×10^{8}	2.82×10^{8}	1.66×10^{9}	
$\theta_{\pi^0\pi^0} < 23°$	77970	3636	1.19×10^{8}	1.02×10^{8}	6.04×10^{8}	
$m_{\pi^0\pi^0} \in (5.212, 5.347)$ GeV	75859	933	5472	1622	8673	0.40% ± 0.01%
$m_{\pi^0\pi^0} \in (5.336, 5.397)$ GeV	2831	2545	2424	473	2248	4.0% ± 0.6%

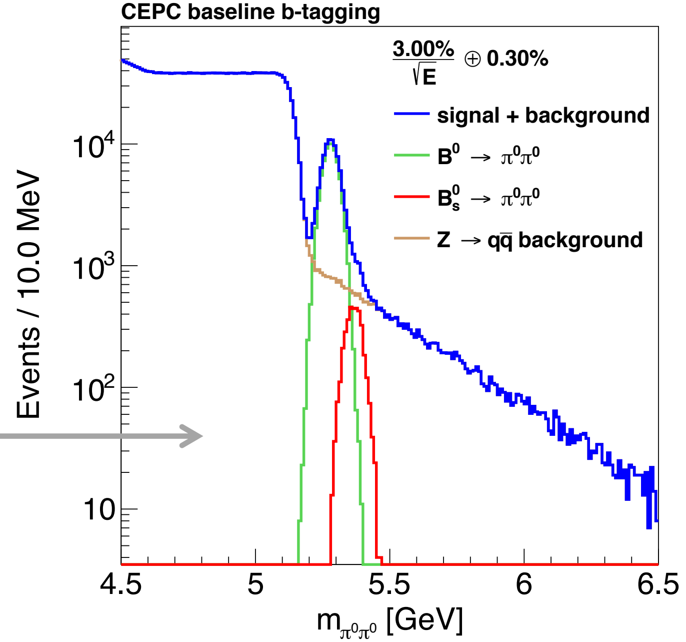

- After b-tagging & π^0 reconstruction
- 4 cuts on energy and angular distributions of π^0 pairs
  - Signal efficiency ~ 40%
  - Background suppression ~ 3 orders of magnitude
- Optimize mass window → minimize accuracy $\sqrt{S+B}/S$
  - ~ 7.5×10^4 $B^0 \to \pi^0\pi^0$, accuracy ~ 0.4%
  - ~ 2.5×10^3 $B^0_s \to \pi^0\pi^0$, accuracy ~ 4.0%

Background components of $B^0_{(s)} \to \pi^0\pi^0$

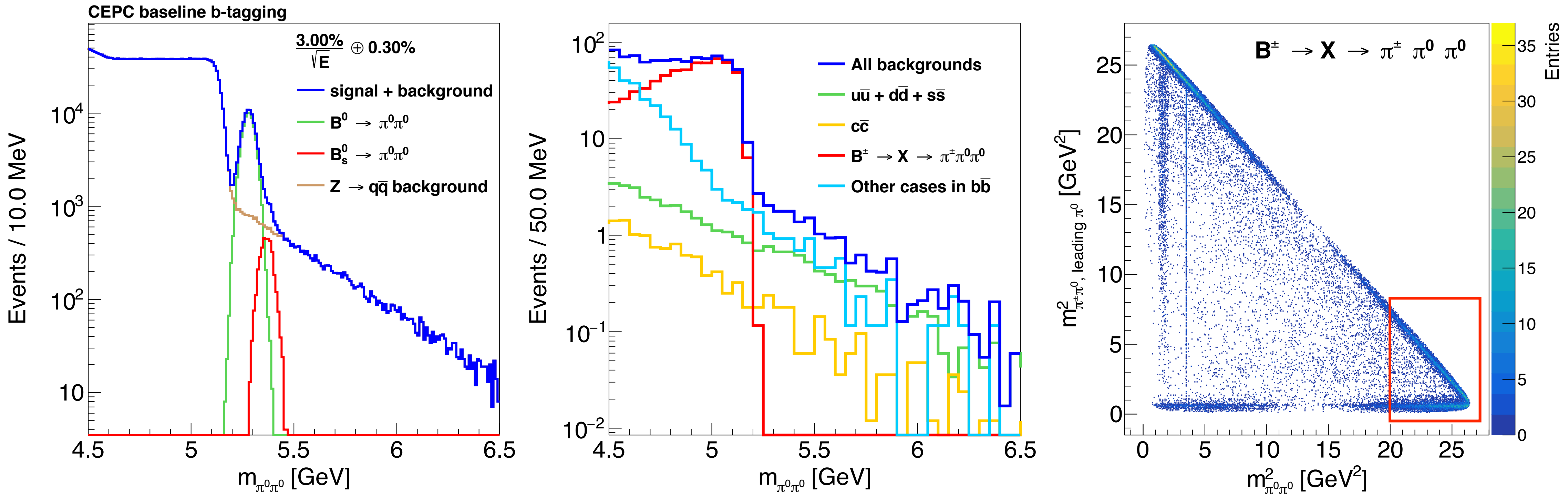

- Step structure mainly from $B^{\pm} \to X \to \pi^{\pm}\pi^0\pi^0$
  - $m^2_{\pi^0\pi^0} > 20\ \mathrm{GeV}^2$
    - $\sim 93\%\ B^{\pm} \to \rho(770)^{\pm}\pi^0, \rho(770)^{\pm} \to \pi^{\pm}\pi^0$
    - $\sim 7\%\ B^{\pm} \to \pi^{\pm}\pi^0\pi^0$
  - Kinematic constraint → cut-off on $m_{\pi^0\pi^0} \sim 5.2$ GeV

Event selection of $B^0_{(s)} \to \eta\eta$

Selection chain	$B^0 \to \eta\eta \to 4\gamma$	$B^0_s \to \eta\eta \to 4\gamma$	$u\bar{u}+d\bar{d}+s\bar{s}$	$c\bar{c}$	$b\bar{b}$	$\sqrt{S+B}/S$
Yield at Tera-Z	1912	47437	4.29×10^{11}	1.20×10^{11}	1.51×10^{11}	
b-tagging	1529	37950	3.64×10^{9}	9.94×10^{9}	1.21×10^{11}	
$\eta \to \gamma\gamma$	1000	25820	2.13×10^{8}	5.60×10^{8}	9.41×10^{9}	
$E_{\eta\eta} > 20$ GeV	934	24158	1.39×10^{7}	1.09×10^{7}	9.46×10^{7}	
$\theta_{\eta\eta} < 30°$	814	21135	6.76×10^{6}	5.68×10^{6}	5.17×10^{7}	
$m_{\eta\eta} \in (5.233, 5.326)$ GeV	693	2103	2328	676	8030	17% $\pm$ 2%
$m_{\eta\eta} \in (5.310, 5.423)$ GeV	155	19208	2184	1014	7388	0.90% $\pm$ 0.05%

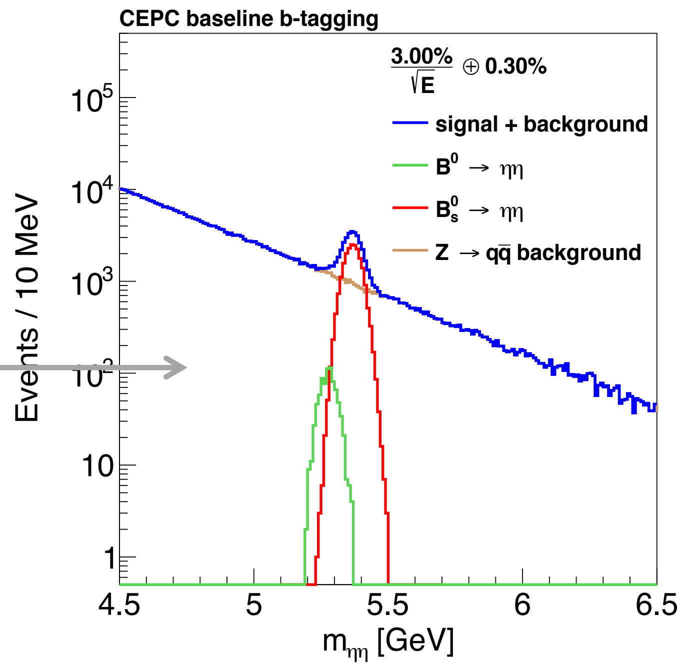

- After b-tagging & η reconstruction
- Cuts on energy and angular distributions of η pairs
  - Signal efficiency ~ 45%
  - Background suppression ~ 5 orders of magnitude
- Optimize mass window → minimize accuracy $\sqrt{S+B}/S$
  - ~ 700 $B^0 \to \eta\eta$, accuracy ~ 17%
  - ~ 2×10^4 $B^0_s \to \eta\eta$, accuracy ~ 0.9%

Other effects

- Photon conversion
  - Central region ~5-10%, Forward region ~25%, ~80% can be recovered
  - Average conversion rate ~3% (each photon)
    $\rightarrow$ 12% efficiency lost of $B^0_{(s)} \rightarrow \pi^0\pi^0, \eta\eta$
- Photon separation (especially di-photon merging)
  - 2cm $\rightarrow$ 80% separation efficiency (CEPC baseline, 5GeV γ)
  - 2cm $\rightarrow$ 10 mrad angular separation (ECAL R_{inner}=2m)
  - Only energetic π^0 suffers
    $\rightarrow$ 10% efficiency lost of $B^0_{(s)} \rightarrow \pi^0\pi^0$

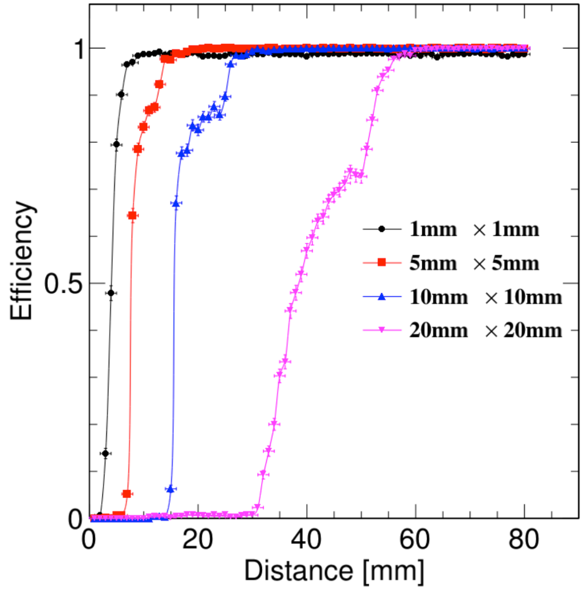

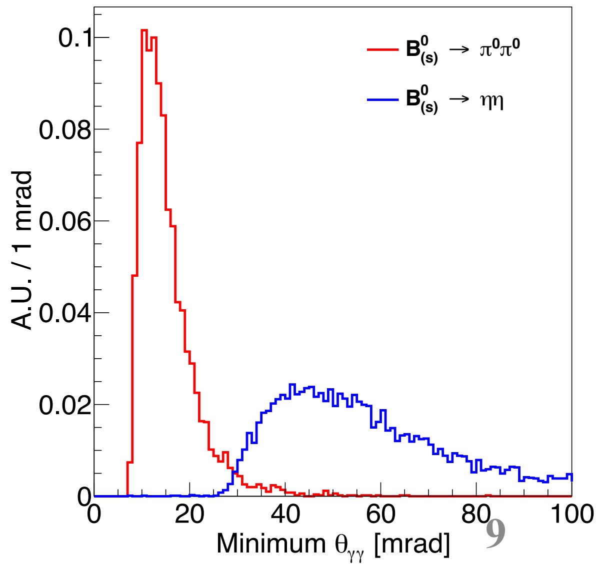

Final realistic results

Channels	$B^0 \rightarrow \pi^0\pi^0$	$B^0_s \rightarrow \pi^0\pi^0$	$B^0 \rightarrow \eta\eta$	$B^0_s \rightarrow \eta\eta$
Signal yield	60000	2000	600	17500
Accuracy	0.45%	4.5%	18%	0.95%

Determination of CKM angle α

- CKM matrix: quark mixing, CP violation
- B^0 decay related triangle relation

$$V_{ub}V_{ud}^* + V_{cb}V_{cd}^* + V_{tb}V_{td}^* = 0,$$

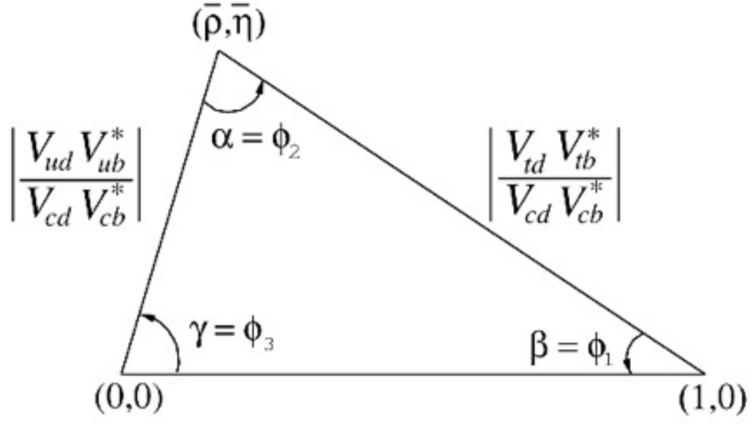

Figure 12.1: Sketch of the unitarity triangle.

$$\beta = \phi_1 = \arg\left(-\frac{V_{cd}V_{cb}^*}{V_{td}V_{tb}^*}\right),$$

$$\alpha = \phi_2 = \arg\left(-\frac{V_{td}V_{tb}^*}{V_{ud}V_{ub}^*}\right),$$

$$\gamma = \phi_3 = \arg\left(-\frac{V_{ud}V_{ub}^*}{V_{cd}V_{cb}^*}\right).$$

- α determination via weak transition b → uud
  - Commonly used decay modes
    - $B \to \rho\rho, \pi\pi, \rho\pi$
  - Both tree and penguin diagrams
  - Penguin contribution is non-negligible
  - Using isospin conservation to deal with penguin pollution

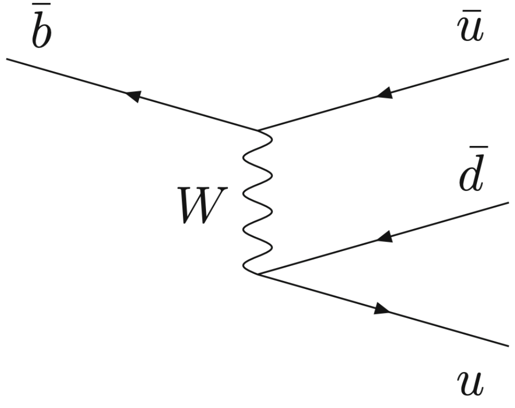

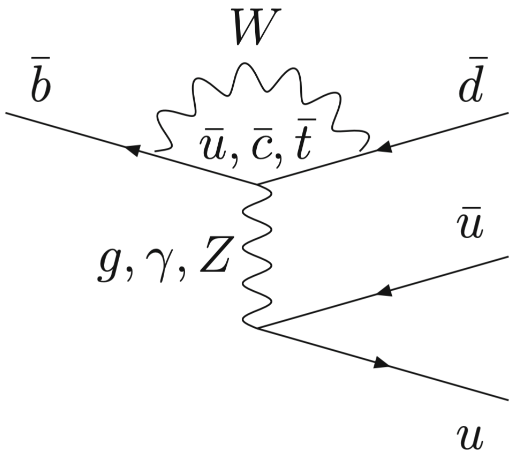

Determination of CKM angle α

Ref. https://inspirehep.net/literature/1598487

Isospin analysis of $B \to \pi\,\pi$: $B^0 \to \pi^+\pi^-, \pi^0\pi^0, B^+ \to \pi^+\pi^0$

- 3 amplitudes can be parameterized by 12 real parameters (complex tree and penguin contributions)
- 6 parameters can be further eliminated by:
  - 2 complex isospin relations (4 real constraints)
  - absence of penguin contribution to $B^+ \to \pi^+\pi^0$ (2 real constraints)
- Remain only 6 degrees of freedom!
- From experimental side
  - 6 observables are available to constrain the 6D parameter space

$$A^{+0} = \frac{1}{\sqrt{2}} A^{+-} + A^{00}$$

$$\bar{A}^{-0} = \frac{1}{\sqrt{2}} \bar{A}^{+-} + \bar{A}^{00}$$

$$\frac{1}{\tau_{B^{i+j}}} \mathcal{B}^{ij} = \frac{|A^{ij}|^2 + |\bar{A}^{ij}|^2}{2},$$

$$\mathcal{C}^{ij} = \frac{|A^{ij}|^2 - |\bar{A}^{ij}|^2}{|A^{ij}|^2 + |\bar{A}^{ij}|^2},$$

$$\mathcal{S}^{ij} = \frac{2\mathcal{I}m(\bar{A}^{ij} A^{ij*})}{|A^{ij}|^2 + |\bar{A}^{ij}|^2},$$

Table 3 World averages for the relevant experimental observables in the $B \to \pi^i\pi^j$ modes: branching fraction $\mathcal{B}^{ij}_{\pi\pi}$, time-integrated CP asymmetry $\mathcal{C}^{ij}_{\pi\pi}$, time-dependent asymmetry $\mathcal{S}^{ij}_{\pi\pi}$ and correlation (ρ)

Observable	World average	References
$\mathcal{B}^{+-}_{\pi\pi}$ ($\times 10^6$)	5.10 ± 0.19	[24–28]
$\mathcal{B}^{+0}_{\pi\pi}$ ($\times 10^6$)	5.48 ± 0.34	[25–27,29]
$\mathcal{B}^{00}_{\pi\pi}$ ($\times 10^6$)	1.59 ± 0.18	[24,30]
$\mathcal{C}^{00}_{\pi\pi}$	-0.34 ± 0.22	[24,30]
$\mathcal{C}^{+-}_{\pi\pi}$	-0.284 ± 0.039	[31–33]
$\mathcal{S}^{+-}_{\pi\pi}$	-0.672 ± 0.043	[31–33]
$\rho(\mathcal{C}^{+-}_{\pi\pi}, \mathcal{S}^{+-}_{\pi\pi})$	$+0.013$	[31–33]

Time-integrated CP asymmetry of $B^0 \to \pi^0\pi^0$

$$A_{CP}^{00}\ (or\ C_{\pi\pi}^{00}) = \frac{\Gamma(B^0 \to \pi^0\pi^0) - \Gamma(\bar{B}^0 \to \pi^0\pi^0)}{\Gamma(B^0 \to \pi^0\pi^0) + \Gamma(\bar{B}^0 \to \pi^0\pi^0)}$$

- b-charge tagging performance:
  - wrong tag fraction, ω
  - tagging efficiency, ϵ_{tag}
  - effective tagging efficiency (power), ϵ_{eff}

$$\epsilon_{eff} = \epsilon_{tag}(1-2\omega)^2$$

- b-charge tagging at CEPC
  - Jet charge measurement at MCTruth level (by Hanhua)
    - infer b-charge by leading charged particles
    - ω ~35%, ϵ_{eff} ~10%
  - Dedicated b-charge tagging algorithm for $B_s \to J/\psi\phi$ (by Mingrui)
    - potential to improve ω ~25%, ϵ_{eff} ~20%
- A_{CP} = -0.33 (W.A.)
  - $\sigma_{A_{CP}}$ = 0.01 ~ 0.006 when ω = 35% ~ 25%

$$A_{CP}^{Measured} = \frac{[\bar{N}(1-\omega)+N\omega]-[\bar{N}\omega+N(1-\omega)]}{\bar{N}+N}$$
$$= (1-2\omega)\frac{\bar{N}-N}{\bar{N}+N} = (1-2\omega)A_{CP}^{Truth}$$

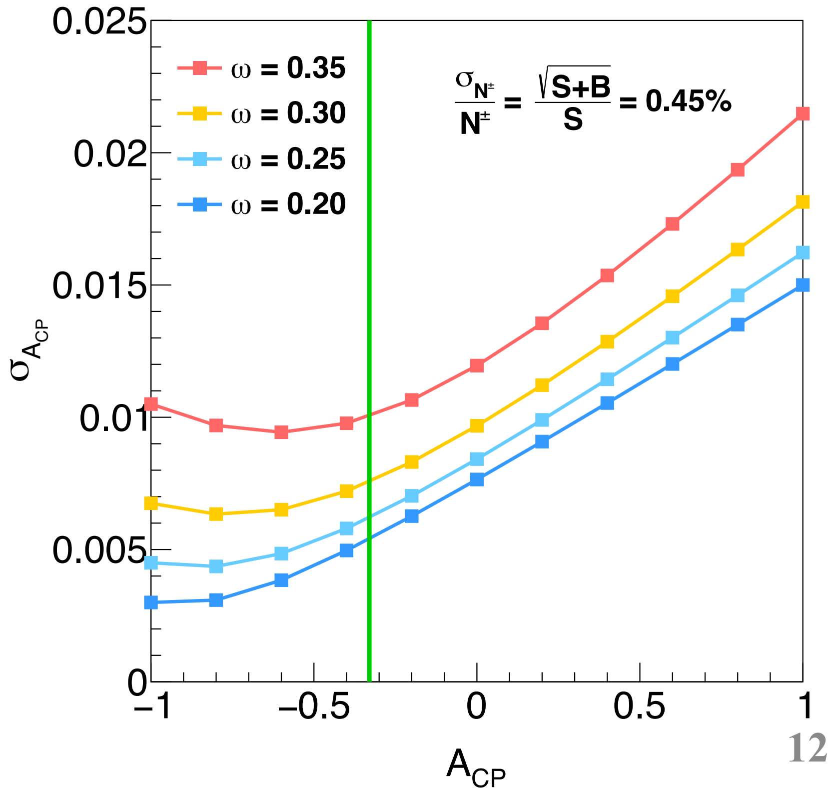

Estimation of other two $B \rightarrow \pi\,\pi$ channels

- Simple method of "efficiency & purity" estimation

$$Accuracy \sim \frac{1}{\sqrt{Yield \times \epsilon \times p}}$$

- Based on the understanding of detector performance
  - Fast simulation results of π^0 (right plot)
  - Much better performance of charged particles

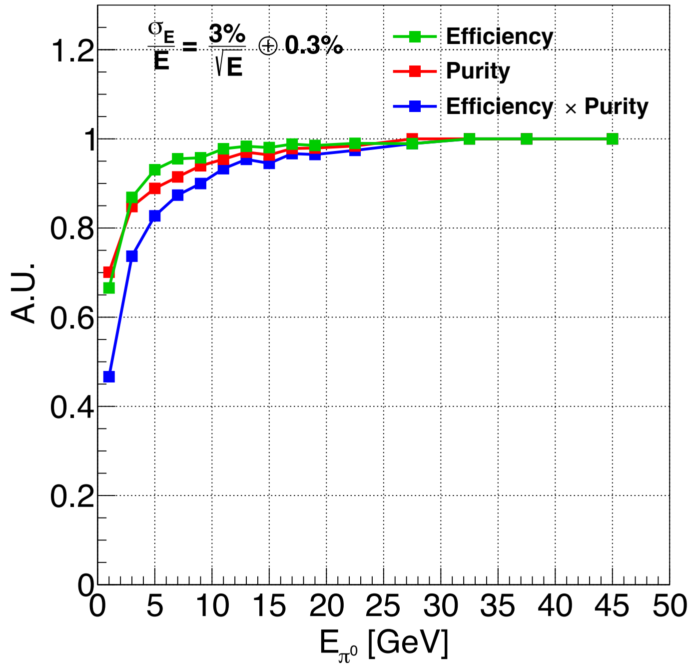

Channel	Branching ratio ($\times 10^{-6}$)	Yield at Tera-Z	Efficiency ϵ	Purity p	$\epsilon \times p$	Relative accuracy
$B^0 \rightarrow \pi^0\pi^0$	1.59	1.9×10^5	40%	80%	32%	0.4%
$B^+ \rightarrow \pi^+\pi^0$	5.5	6.6×10^5	65%	85%	55%	0.16%
$B^0 \rightarrow \pi^+\pi^-$	5.12	6.3×10^5	90%	85%	77%	0.15%

Input parameters to determine α

- Uncertainty on the CP asymmetry of $B^0 \to \pi^+\pi^-$
  - $\sigma_{A^{+-}}$ use the same method as $\sigma_{A^{00}}$: ~ 0.0021
  - $\sigma_{S^{+-}}$ is rescaled by assuming $\sigma_{A^{+-}}/\sigma_{S^{+-}}$ is same as LHCb: ~ 0.0018

	Belle II		Tera-Z	
	Central value	Uncertainty	PDG central value	Statistical uncertainty
B00	1.31E-06	±0.03(2.3%)±0.03	1.59E-06	0.45%
B+-	5.04E-06	±0.03(0.6%)±0.08	5.12E-06	0.15%
B+0	5.86E-06	±0.03(0.5%)±0.09	5.5E-06	0.16%
A00	-0.14	±0.03±0.01	-0.33	±0.006
A+-	-0.33	±0.01±0.03	-0.32	±0.0021
S+-	-0.64	±0.01±0.01	-0.65	±0.0018
ω	23%	-	25%	-
Effective tagging efficiency (power)	30%	-	25%	-

Fitting results of α

Ref. https://inspirehep.net/literature/1598487

Isospin analysis

- $B \to \pi\pi$ system only (by Lingfeng)
  - Scan of confidence level for fitting α
  - 1σ confidence level interval of α
    - Full Belle II
      - [97.1°, 100.3°] = 3.2°
    - Belle II + CEPC (Tera-Z)
      - Only $B^0 \to \pi^0\pi^0$ updated to CEPC
      - [97.7°, 99.8°] = 1.9°
    - Full CEPC (Tera-Z)
      - [98.6°, 99.1°] = 0.5°

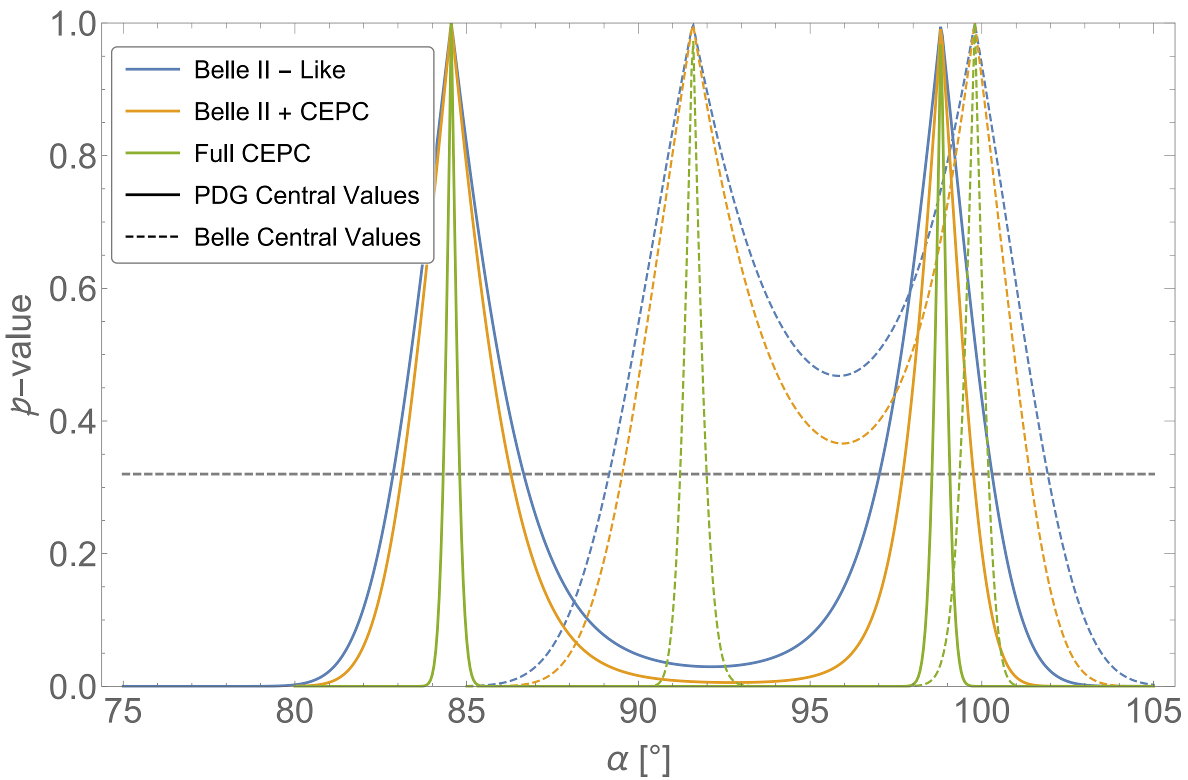

- CKM global fit (by Pro. Sébastien & Olivier)
  - Please see the talk in the second flavor session

16:00 **Potential impact of CEPC on the extraction of the CKM angle alpha** *25′*
Speaker: Dr. Sébastien Descotes-Genon

Time-dependent CP asymmetry of $B^0 \to \pi^0\pi^0$: $S^{00}_{\pi\pi}$

- Extra constraint of $S^{00}_{\pi\pi}$ can reduce the two-fold ambiguity on the solutions of α in [75, 105]°
- Time-dependent analysis need vertex information
  - $\pi^0 \to e^+e^-\gamma$ Dalitz decay or photon conversion events
  - Belle II: 147 Dalitz events & 124 photon conversion events

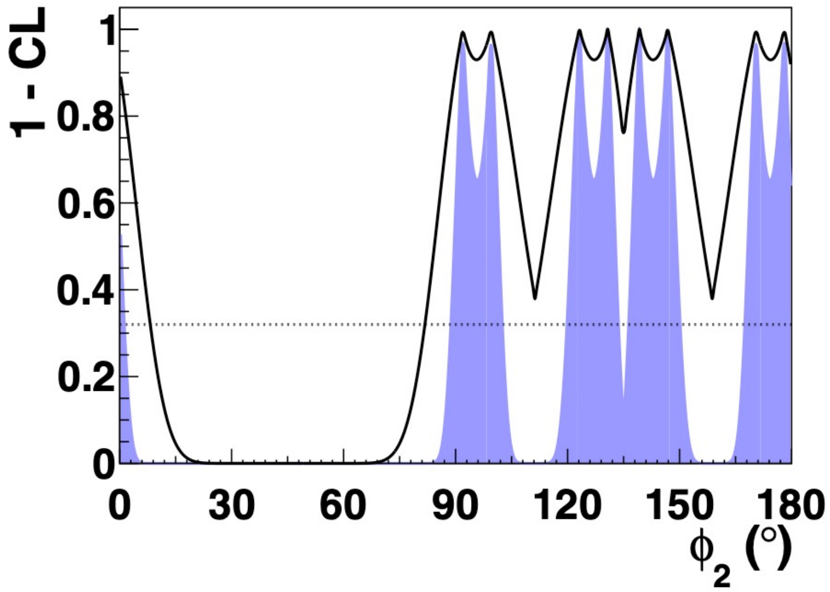

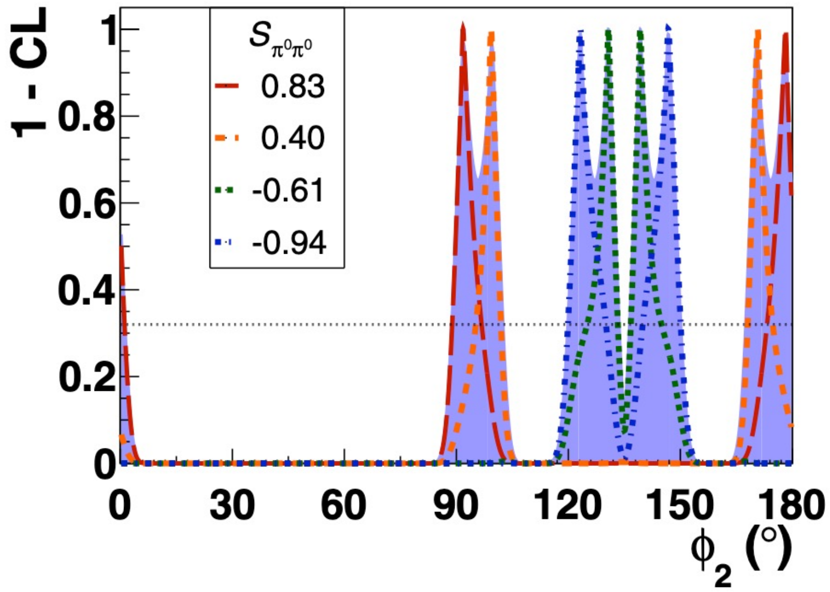

- CEPC advantage
  - Larger boost of B meson
  - Decent vertex reconstruction
  - B decay lifetime resolution ~ 15 fs

Future work…

Summary

- Charmless two-body hadronic B-meson decays: $B_{(s)}^{0} \rightarrow \pi^0\pi^0, \eta\eta$
  - CKM angle α determination

- Fast simulation: key detector performance modeling
  - b-tagging: $\varepsilon \sim 80\%,\ p \sim 90\%$
  - EM resolution: $3\%/\sqrt{E} \oplus 0.3\%$ (σ_{m_B}~ 30MeV)
  - Other effects: photon conversion & separation
- Anticipated performance

Channels	$B^0 \rightarrow \pi^0\pi^0$	$B_s^0 \rightarrow \pi^0\pi^0$	$B^0 \rightarrow \eta\eta$	$B_s^0 \rightarrow \eta\eta$
Signal yield	60000	2000	600	17500
Accuracy	0.45%	4.5%	18%	0.95%

Summary

- Determination of CKM angle α
  - $B \rightarrow \pi\pi$ system only (this talk)
    - Estimate anticipated uncertainties on BR and CP asymmetry at CEPC
      - Final state ($\pi^0, \pi^{\pm}$) reconstruction ϵ & p
      - b-charge tagging: ω = 35% ~ 25%, ϵ_{eff} = 10% ~ 20%
    - Isospin analysis: 1σ confidence level interval of α
      - Full Belle II [97.1°, 100.3°] = 3.2°
      - Full CEPC [98.6°, 99.1°] = 0.5°, ~ 6 times better than Belle II
  - Global fit → Pro. Sébastien's talk

- Future work
  - Time-dependent analysis of $B^0 \rightarrow \pi^0\pi^0$ ($S_{\pi\pi}^{00}$) to reduce ambiguity on α
    - $\pi^0 \rightarrow e^+e^-\gamma$ Dalitz decay
    - photon conversion events

Thank you!

More precise determination of α using $B \to \rho\,\rho$

- More precise than $B \to \pi\,\pi$ modes
  - Larger branching ratios than $B \to \pi\,\pi$
  - $B^0 \to \rho^0\rho^0$ enjoys the charged final state $\rho^0 \to \pi^+\pi^-$
    - Much better charged particle reconstruction performance than neutral particle
    - $S^{00}_{\rho\rho}$ is accessible to reduce the ambiguity solutions

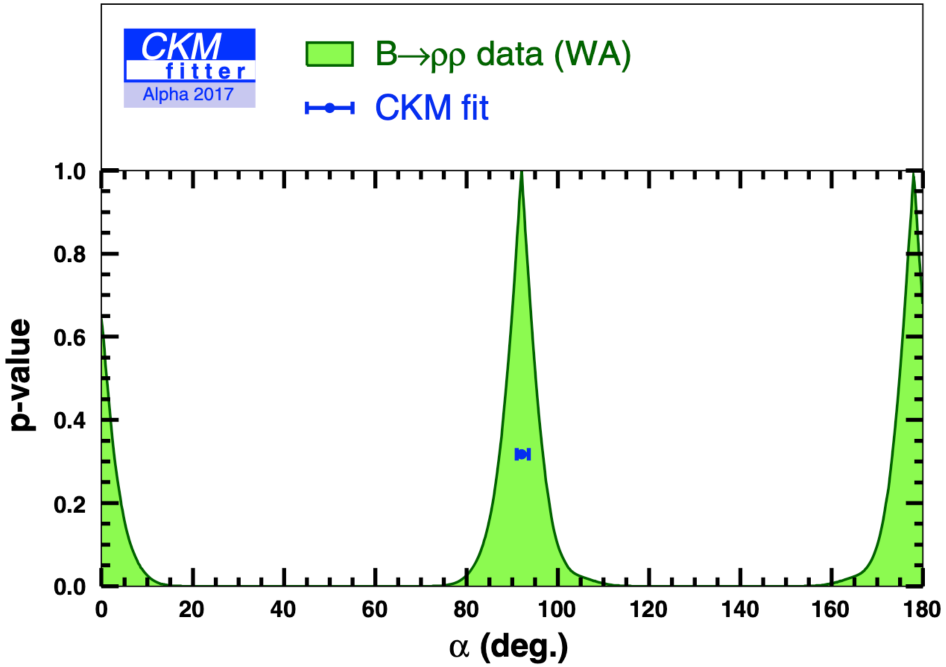

Table 4 World averages for the relevant experimental observables in the $B \to \rho^i \rho^j$ modes: branching fraction $\mathcal{B}^{ij}_{\rho\rho}$, fraction of longitudinal polarisation f^{ij}_L, time-integrated CP asymmetry $\mathcal{C}^{ij}_{\rho\rho}$, time-dependent asymmetry $\mathcal{S}^{ij}_{\rho\rho}$ and correlation (ρ)

Observable	World average
$\mathcal{B}^{+-}_{\rho\rho} \times f^{+-}_L$ ($\times 10^6$)	$(27.76 \pm 1.84) \times (0.990 \pm 0.020)$
$\mathcal{B}^{+0}_{\rho\rho} \times f^{+0}_L$ ($\times 10^6$)	$(24.9 \pm 1.9) \times (0.950 \pm 0.016)$
$\mathcal{B}^{00}_{\rho\rho} \times f^{00}_L$ ($\times 10^6$)	$(0.93 \pm 0.14) \times (0.71 \pm 0.06)$
$\mathcal{C}^{+-}_{\rho_L\rho_L}$	-0.00 ± 0.09
$\mathcal{S}^{+-}_{\rho_L\rho_L}$	-0.15 ± 0.13
$\rho(C^{+-}_{\rho_L\rho_L}, S^{+-}_{\rho_L\rho_L})$	$+0.0002$
$\mathcal{C}^{00}_{\rho_L\rho_L}$	0.2 ± 0.9
$\mathcal{S}^{00}_{\rho_L\rho_L}$	0.3 ± 0.7

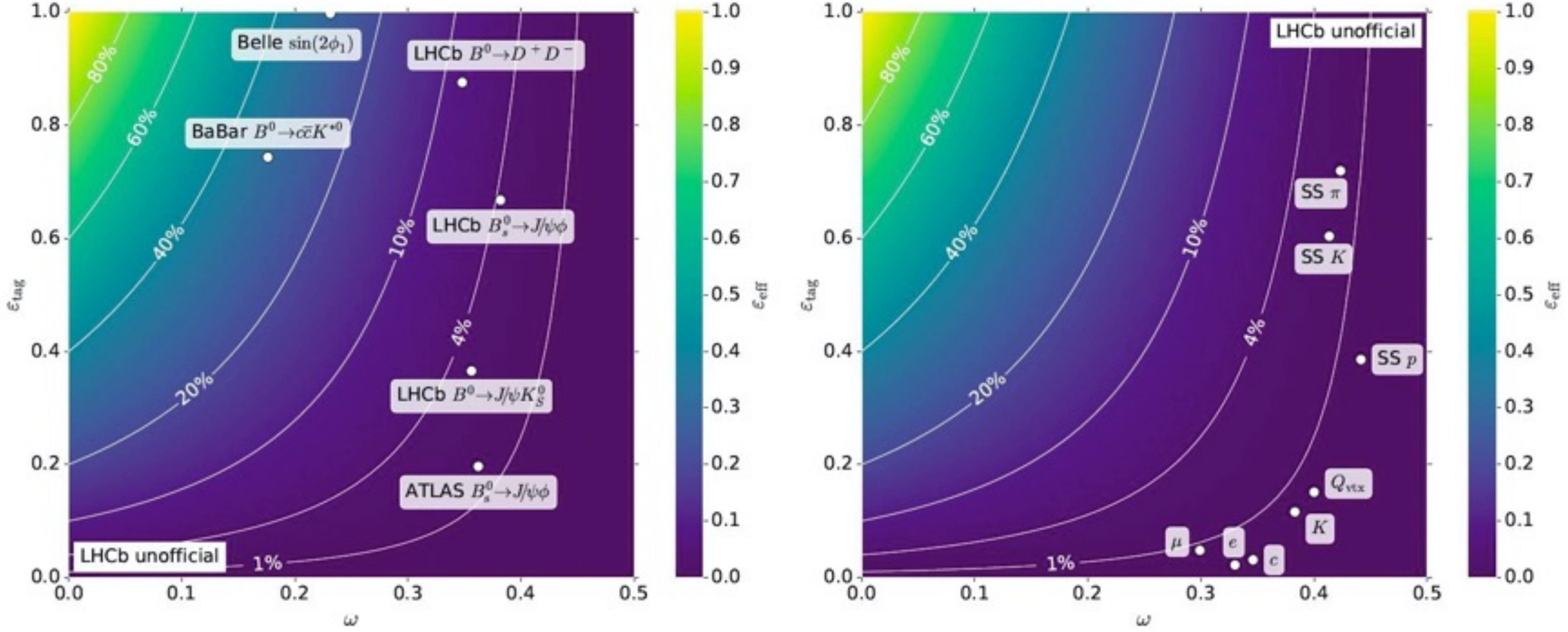

Figure 3.1: Effective tagging efficiency of (left) different HEP experiments and (right) LHCb flavour tagging algorithms [40]. The white lines indicate contours of constant tagging power.

Table 90. Statistical uncertainties $\Delta A_{\pi^0\pi^0}$, $\Delta S_{\pi^0\pi^0}$, and $\Delta\mathcal{B}_{\pi^0\pi^0}/\mathcal{B}_{\pi^0\pi^0}$ for different input values of $A_{\pi^0\pi^0}$ and $S_{\pi^0\pi^0}$ used for the generation of signal MC.

Input values		Time-dependent		Time-integrated	
$A_{\pi^0\pi^0}$	$S_{\pi^0\pi^0}$	$\Delta A_{\pi^0\pi^0}$	$\Delta S_{\pi^0\pi^0}$	$\Delta A_{\pi^0\pi^0}$	$\Delta\mathcal{B}_{\pi^0\pi^0}/\mathcal{B}_{\pi^0\pi^0}$ [%]
0.34 [650]	0.65 [650]	0.22	0.28	0.03	2.2
0.43 [88]	0.79	0.23	0.29	0.03	2.2
0.14 [712]	0.83	0.21	0.26	0.03	2.4
0.14 [712]	0.40	0.20	0.29	0.03	2.3
0.14 [712]	−0.61	0.22	0.27	0.03	2.3
0.14 [712]	−0.94	0.22	0.28	0.03	2.4

Table 91. Branching fractions and CP asymmetry parameters entering in the isospin analysis of the $B \to \pi\pi$ system: Belle measurements at 0.8 ab^{-1} together with the expected Belle II sensitivity at 50 ab^{-1}.

	Value	0.8 ab^{-1}	50 ab^{-1}
$\mathcal{B}_{\pi^+\pi^-}$ [10^{-6}]	5.04	$\pm 0.21 \pm 0.18$ [727]	$\pm 0.03 \pm 0.08$
$\mathcal{B}_{\pi^0\pi^0}$ [10^{-6}]	1.31	$\pm 0.19 \pm 0.19$ [712]	$\pm 0.03 \pm 0.03$
$\mathcal{B}_{\pi^+\pi^0}$ [10^{-6}]	5.86	$\pm 0.26 \pm 0.38$ [727]	$\pm 0.03 \pm 0.09$
$A_{\pi^+\pi^-}$	0.33	$\pm 0.06 \pm 0.03$ [728]	$\pm 0.01 \pm 0.03$
$S_{\pi^+\pi^-}$	−0.64	$\pm 0.08 \pm 0.03$ [728]	$\pm 0.01 \pm 0.01$
$A_{\pi^0\pi^0}$	0.14	$\pm 0.36 \pm 0.10$ [712]	$\pm 0.03 \pm 0.01$

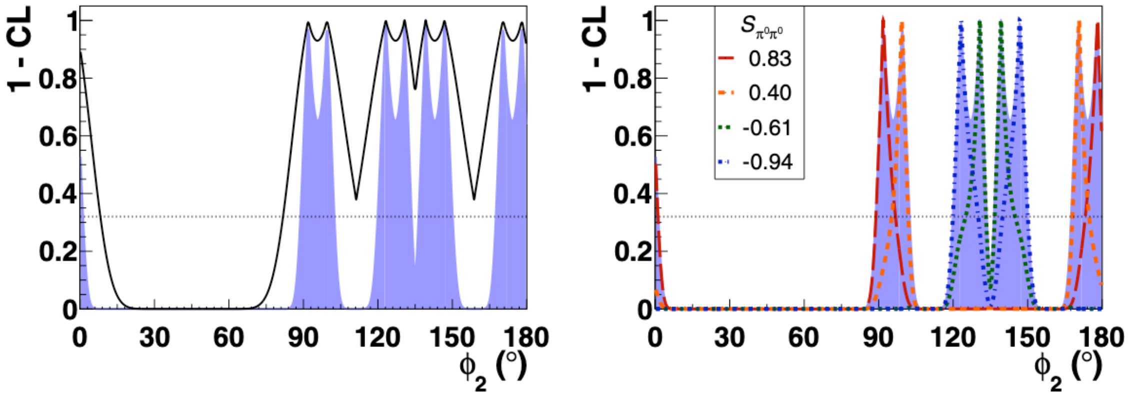

Fig. 116. Scan of the confidence for ϕ_2 performing isospin analysis of the $B \to \pi\pi$ system. (Left): The black solid line shows the result of the scan using data from Belle measurements (see Table 91). The blue shaded area in both plots shows the projection for Belle II. (Right): Results of the scan adding the $S_{\pi^0\pi^0}$ constraint. Each line shows the result for a different $S_{\pi^0\pi^0}$ value. The dotted horizontal lines correspond to $1\,\sigma$.

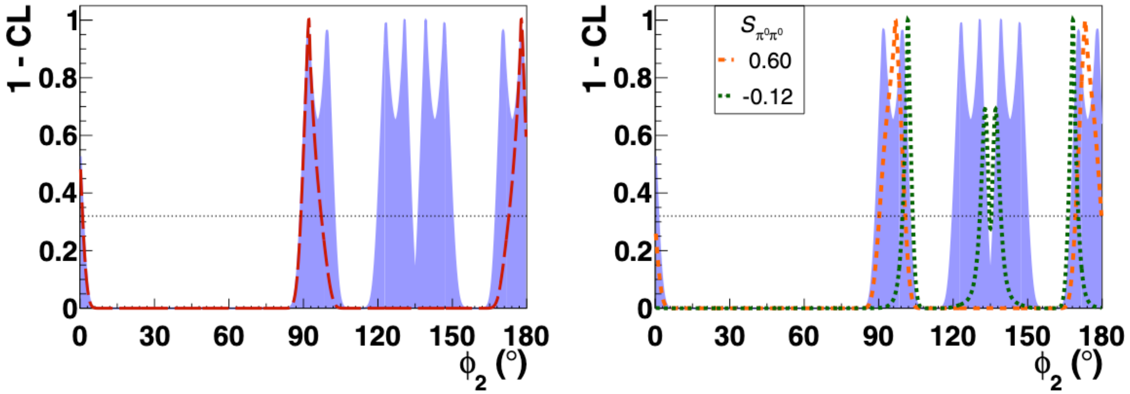

Fig. 117. Scan of the confidence for ϕ_2 performing isospin analysis of the $B \to \pi\pi$ system. The blue shaded area in both plots shows the projection of the Belle measurements (see Fig. 116) for Belle II. Results of the scan with additional $S_{\pi^0\pi^0}$ constraints are shown by dashed lines. Each line correspond to different input $S_{\pi^0\pi^0}$ values. The red long dashed line on the left figure shows the result for $S_{\pi^0\pi^0} = 0.83$. The dotted horizontal line correspond to $1\,\sigma$.

N_sig = 60000, Accuracy = 0.45%

ω	0.35	0.30	0.25	0.20
Acp = -0.33 (PDG)	0.010	0.008	0.006	0.005
Acp = -0.14 (Belle)	0.011	0.009	0.007	0.007

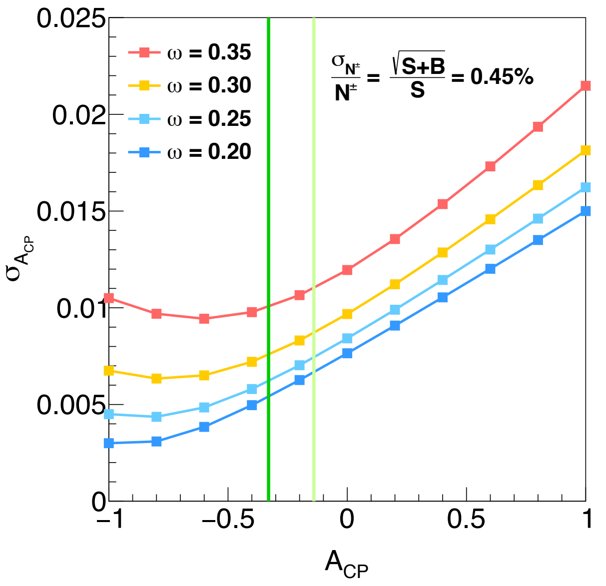

B0→π+π-, N_sig = 614400*90% = 5.5E5, Accuracy = 0.15%

ω	0.35	0.30	0.25	0.20
Acp = -0.32 (PDG)	0.0034	0.0025	0.0021	0.0018
Acp = -0.33 (Belle)	0.0033	0.0025	0.0021	0.0018

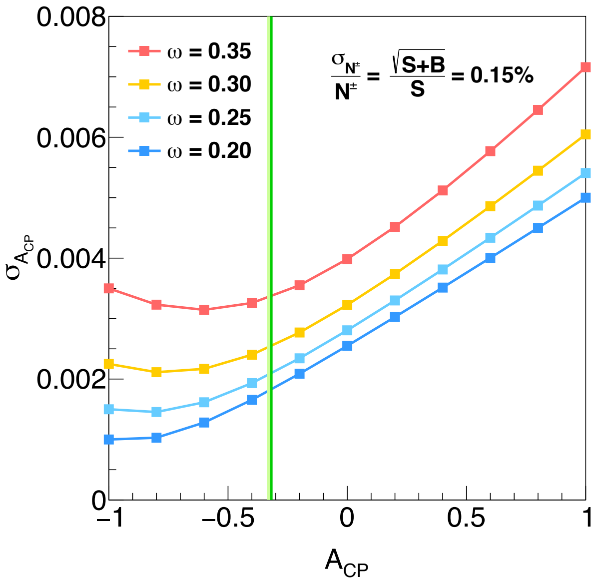

Data sample	$C_{\pi^+\pi^-}$	$S_{\pi^+\pi^-}$
Run 1 ($3\,\text{fb}^{-1}$ [112])	$-0.34 \pm 0.06 \pm 0.01$	$-0.63 \pm 0.05 \pm 0.01$
Run 1-3 ($23\,\text{fb}^{-1}$)	0.015	0.013
Run 1-6 ($300\,\text{fb}^{-1}$)	0.004	0.004

$$N^{\pm} = N^{+}_{Truth} + N^{-}_{Truth} = N^{+}_{Reco} + N^{-}_{Reco}$$

$$\sigma_{N^{\pm}} = accuracy \times N^{\pm}$$

Define ratio r

$$N^{+}_{Reco} = rN^{\pm}$$
$$N^{-}_{Reco} = (1-r)N^{\pm}$$

$$\sigma_{N^{+}_{Reco}} = r\sigma_{N^{\pm}}$$
$$\sigma_{N^{-}_{Reco}} = (1-r)\sigma_{N^{\pm}}$$

$$\begin{pmatrix} N^{+}_{Reco} \\ N^{-}_{Reco} \end{pmatrix} = \begin{pmatrix} 1-\omega & \omega \\ \omega & 1-\omega \end{pmatrix} \begin{pmatrix} N^{+}_{Truth} \\ N^{-}_{Truth} \end{pmatrix}$$

$$\begin{pmatrix} N^{+}_{Truth} \\ N^{-}_{Truth} \end{pmatrix} = \begin{pmatrix} \frac{\omega-1}{2\omega-1} & \frac{\omega}{2\omega-1} \\ \frac{\omega}{2\omega-1} & \frac{\omega-1}{2\omega-1} \end{pmatrix} \begin{pmatrix} N^{+}_{Reco} \\ N^{-}_{Reco} \end{pmatrix}$$

$$N^{+}_{Truth} = \frac{\omega-1}{2\omega-1} \times N^{+}_{Reco} + \frac{\omega}{2\omega-1} \times N^{-}_{Reco}$$

$$N^{-}_{Truth} = \frac{\omega}{2\omega-1} \times N^{+}_{Reco} + \frac{\omega-1}{2\omega-1} \times N^{-}_{Reco}$$

$$\begin{aligned} \sigma^2_{N^{+}_{Truth}} &= (\frac{\partial N^{+}_{Truth}}{\partial N^{+}_{Reco}})^2 \sigma^2_{N^{+}_{Reco}} + (\frac{\partial N^{+}_{Truth}}{\partial N^{-}_{Reco}})^2 \sigma^2_{N^{-}_{Reco}} \\ &= [\frac{\omega-1}{2\omega-1} \times r \times \sigma_{N^{\pm}}]^2 + [\frac{\omega}{2\omega-1} \times (1-r) \times \sigma_{N^{\pm}}]^2 \end{aligned}$$

$$\begin{aligned} \sigma^2_{N^{-}_{Truth}} &= (\frac{\partial N^{-}_{Truth}}{\partial N^{+}_{Reco}})^2 \sigma^2_{N^{+}_{Reco}} + (\frac{\partial N^{-}_{Truth}}{\partial N^{-}_{Reco}})^2 \sigma^2_{N^{-}_{Reco}} \\ &= [\frac{\omega}{2\omega-1} \times r \times \sigma_{N^{\pm}}]^2 + [\frac{\omega-1}{2\omega-1} \times (1-r) \times \sigma_{N^{\pm}}]^2 \end{aligned}$$

$$A_{CP} = \frac{N^{+}_{Truth} - N^{-}_{Truth}}{N^{+}_{Truth} + N^{-}_{Truth}} = \frac{N^{+}_{Truth} - (N^{\pm} - N^{+}_{Truth})}{N^{\pm}} = \frac{2N^{+}_{Truth} - N^{\pm}}{N^{\pm}} = 2\frac{N^{+}_{Truth}}{N^{\pm}} - 1$$

$$\begin{aligned} \sigma^2_{A_{CP}} &= (\frac{\partial A_{CP}}{\partial N^{+}_{Truth}})^2 \sigma^2_{N^{+}_{Truth}} + (\frac{\partial A_{CP}}{\partial N^{\pm}})^2 \sigma^2_{N^{\pm}} \\ &= [\frac{2}{N^{\pm}}]^2 \sigma^2_{N^{+}_{Truth}} + [\frac{-2N^{+}}{N^{\pm 2}}]^2 \sigma^2_{N^{\pm}} \end{aligned}$$

$B^0 \to \pi^0\pi^0$	Final state	Total in theory	In acceptance	Selected	Efficiency	Purity	Relative accuracy
Tera-Z	$\pi\pi$	195692	-	-	-	-	-
	$\pi_{\gamma\gamma}\pi_{\gamma\gamma}$	191113*0.65 = 124223	-	75859 49689	0.4	0.8 0.72	0.4% 0.5%
	$\pi_{dal}\pi_{\gamma\gamma}$	4579	-	?	?		
	$\pi_{\gamma c\gamma}\pi_{\gamma\gamma}$	191113*0.2 = 38222	-	?	?		
Belle II	$\pi\pi$	103000	-	-	-	-	-
	$\pi_{\gamma\gamma}\pi_{\gamma\gamma}$	100590 - 9270 = 91320	78486	15068	0.192	0.158	2%
	$\pi_{dal}\pi_{\gamma\gamma}$	2410	2060	147	0.072	0.176	
	$\pi_{\gamma c\gamma}\pi_{\gamma\gamma}$	100590*0.09 = 9270	3090	124	0.042		

$\pi^0_{\gamma\gamma}$ are used for the time-integrated CP violation study. There is no event overlap between events with $B^0_{\rm sig}$ candidates reconstructed from two $\pi^0_{\gamma\gamma}$ and events containing Dalitz decays or converted photons.

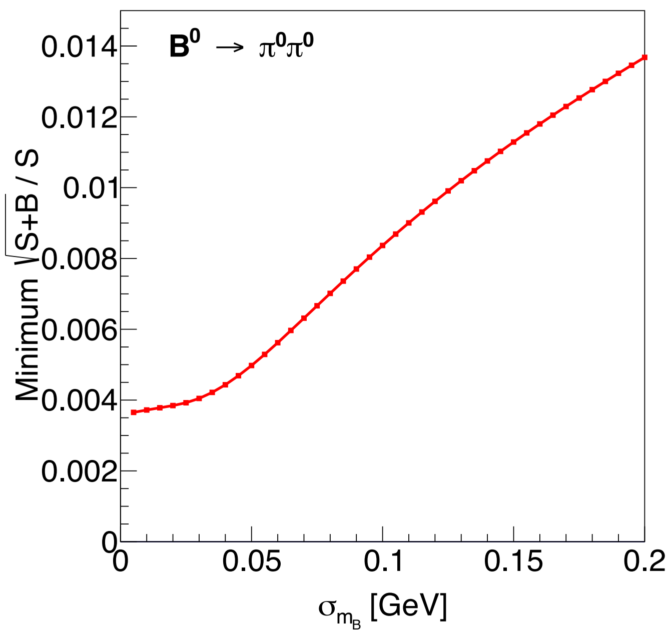

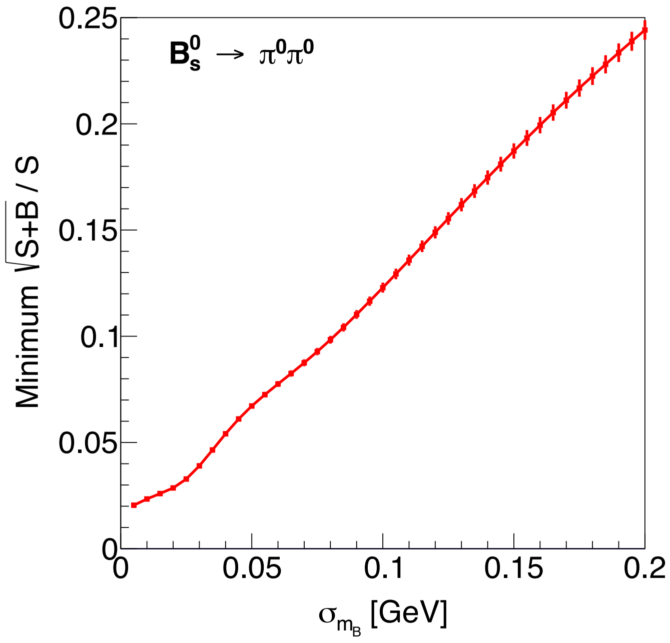

ECAL energy resolution	Channel	σ_{m_B} (MeV)	Signal	$q\bar{q}$ background	Background with false $\pi^0(\eta)$	$\sqrt{S+B}/S$ (%)
$\frac{3\%}{\sqrt{E}} \oplus 0.3\%$	$B^0 \to \pi^0\pi^0$	30.25	75859	15767	7.52%	0.40 ± 0.01
	$B_s^0 \to \pi^0\pi^0$	30.21	2545	5145	14.73%	4.03 ± 0.55
	$B^0 \to \eta\eta$	33.30	693	11034	52.86%	17 ± 2
	$B_s^0 \to \eta\eta$	33.26	19208	10586	65.25%	0.90 ± 0.05
$\frac{17\%}{\sqrt{E}} \oplus 1\%$	$B^0 \to \pi^0\pi^0$	166	57746	381331	4.04%	1.15 ± 0.03
	$B_s^0 \to \pi^0\pi^0$	165	2243	142716	5.74%	19.3 ± 0.6
	$B^0 \to \eta\eta$	170	324	68243	88.27%	85 ± 6
	$B_s^0 \to \eta\eta$	174	8300	49248	86.30%	2.90 ± 0.20

Table 8: Measurement accuracies of $B^0_{(s)} \to \pi^0\pi^0$ and $B^0_{(s)} \to \eta\eta$ at different ECAL energy resolutions when using the CEPC baseline b-tagging.

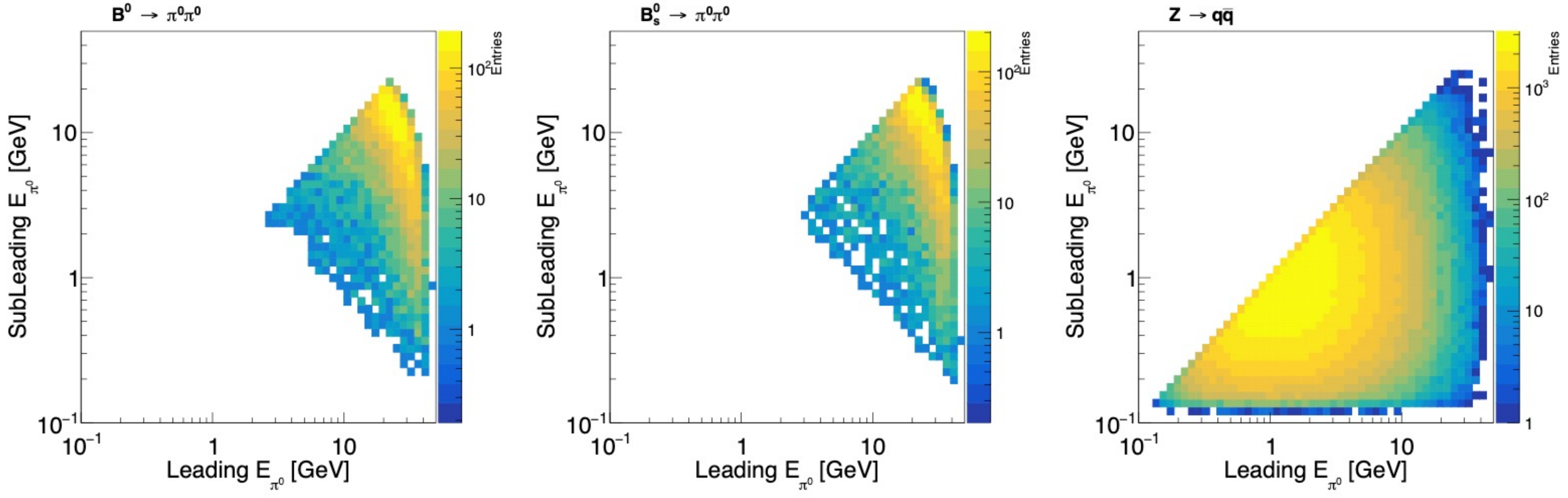

(a) 2D energy spectrum of π^0 pairs in $B^0 \to \pi^0\pi^0$ (left), $B_s^0 \to \pi^0\pi^0$ (middle), and $Z \to q\bar{q}$ (right) events.

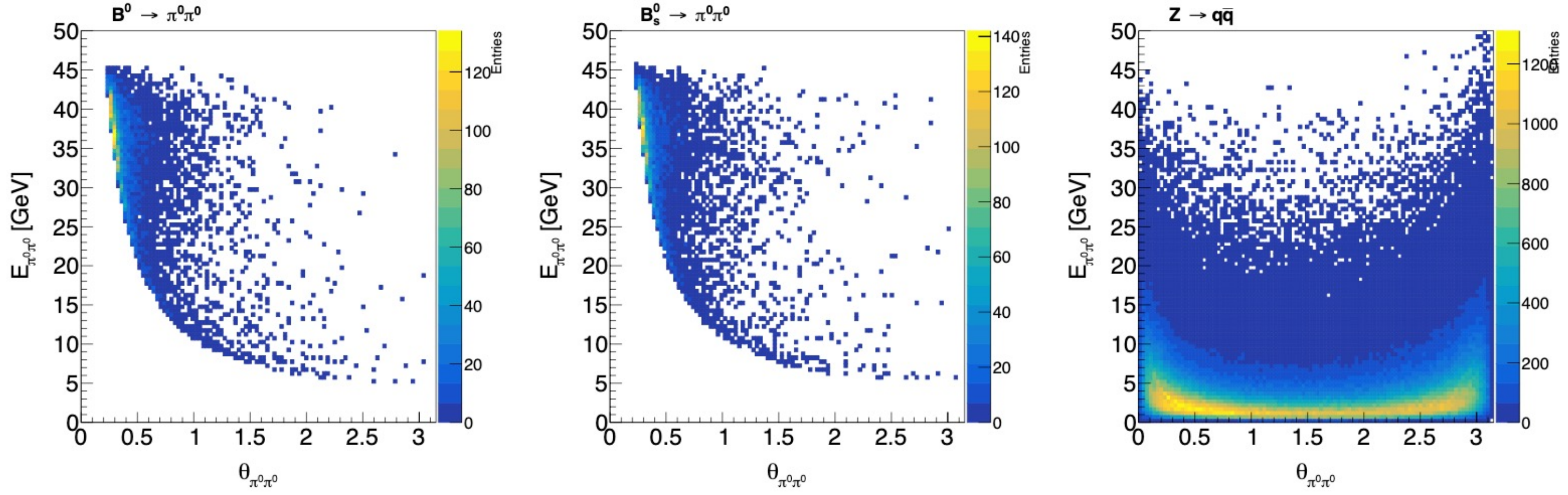

(b) Correlation between $E_{\pi^0\pi^0}$ and $\theta_{\pi^0\pi^0}$ in $B^0 \to \pi^0\pi^0$ (left), $B_s^0 \to \pi^0\pi^0$ (middle), and $Z \to q\bar{q}$ (right) events.

Dependence of B mass resolution on detector performance

ECAL energy resolution

$$\frac{\sigma_E}{E} = \frac{A}{\sqrt{E}} \oplus C$$

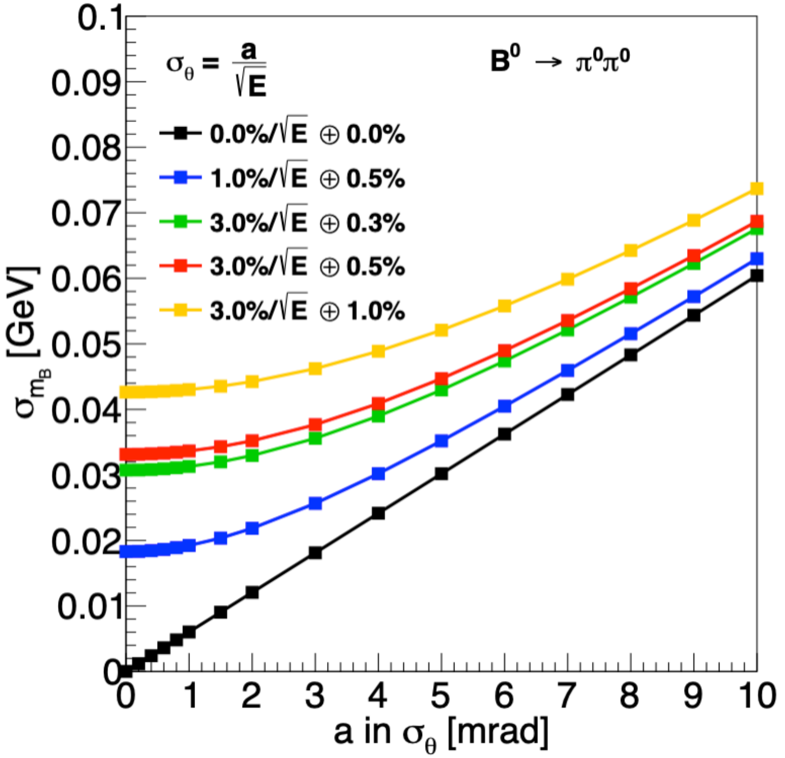

Photon angular resolution

$$\sigma_\theta = \frac{a}{\sqrt{E}}, \ \sigma_\phi = \frac{\sigma_\theta}{sin\theta}$$

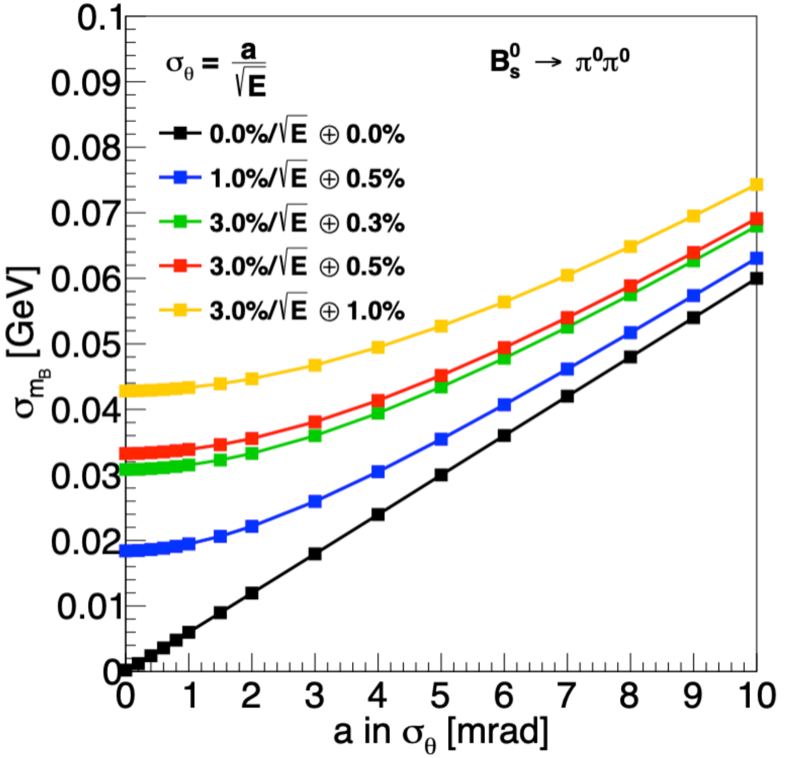

- **CEPC baseline single photon angular resolution ~1mrad/√E**
- **ECAL energy resolution dominates the contribution when σ_θ < 1mrad/√E**
- **The following analysis only takes ECAL energy resolution into account**
- **σ_{mB} ~30 MeV requires ECAL energy resolution ~3%/√E⊕0.3%**

EM Energy Resolution

From a historical perspective

LEP - L3, BGO	LHC - CMS, PbWO4	DAMPE, BGO

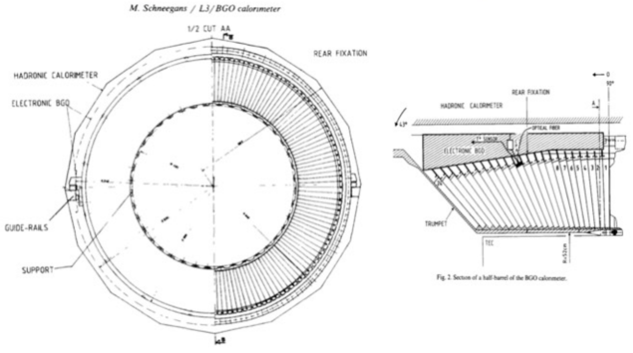

Fig 3 r/φ section of the barrel.

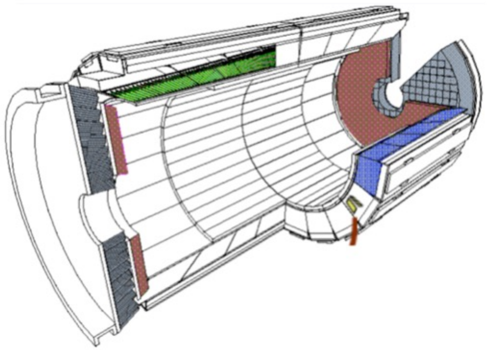

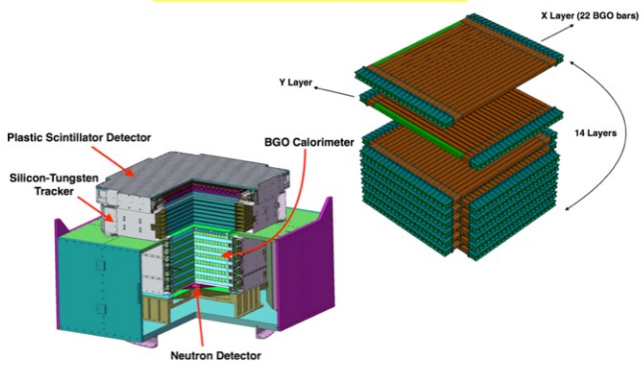

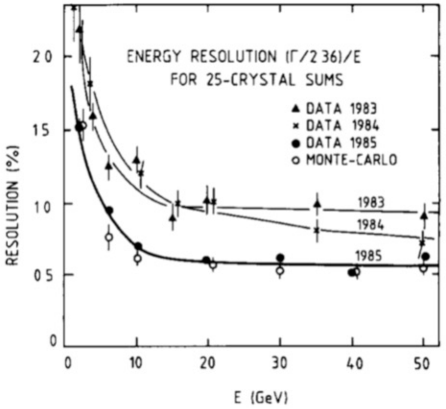

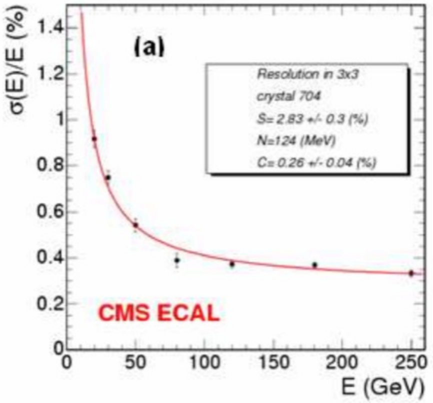

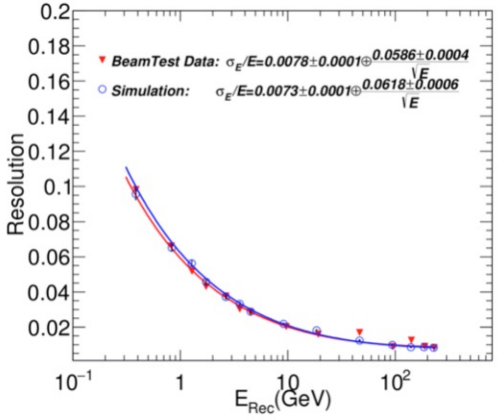

< 2% at 1GeV

The performance now measured in electron beams with final prototypes shows that we are below 2% energy resolution at 1 GeV and near to 5% at 100 MeV.

$2.8\%/\sqrt{E} \oplus 0.3\%$

$5.86\%/\sqrt{E} \oplus 0.78\%$

Belle II ECAL

The intrisic energy resolution of the calorimeter, as measured in a prototype [3], can be approximated as:

$$\frac{\sigma_E}{E} = \sqrt{\left(\frac{0.066\%}{E}\right)^2 + \left(\frac{0.81\%}{\sqrt[4]{E}}\right)^2 + (1.34\%)^2}, \tag{9.1}$$

where E is in GeV and the first term represents the electronics noise contribution.

3.5. *Electromagnetic calorimeter (ECL)*

The electromagnetic calorimeter is used to detect gamma rays as well as to identify electrons, i.e. separate electrons from hadrons, in particular pions. It is a highly segmented array of thallium-doped caesium iodide CsI(Tl) crystals assembled in a projective geometry (Fig. 3). All three detector regions, the barrel as well as the forward and backward endcaps, are instrumented with a total of 8736 crystals, covering about 90% of the solid angle in the centre-of-mass system. The CsI(Tl) crystals, preamplifiers, and support structures have been reused from Belle, whereas the readout electronics and reconstruction software have been upgraded. In the Belle experiment, the energy resolution observed with the same calorimeter was $\sigma_E/E = 4\%$ at 100 MeV, 1.6% at 8 GeV, and the angular resolution was 13 mrad (3 mrad) at low (high) energies; π^0 mass resolution was 4.5 MeV/c^2 [2]; in the absence of background a very similar performance would also be expected for Belle II.

Belle II

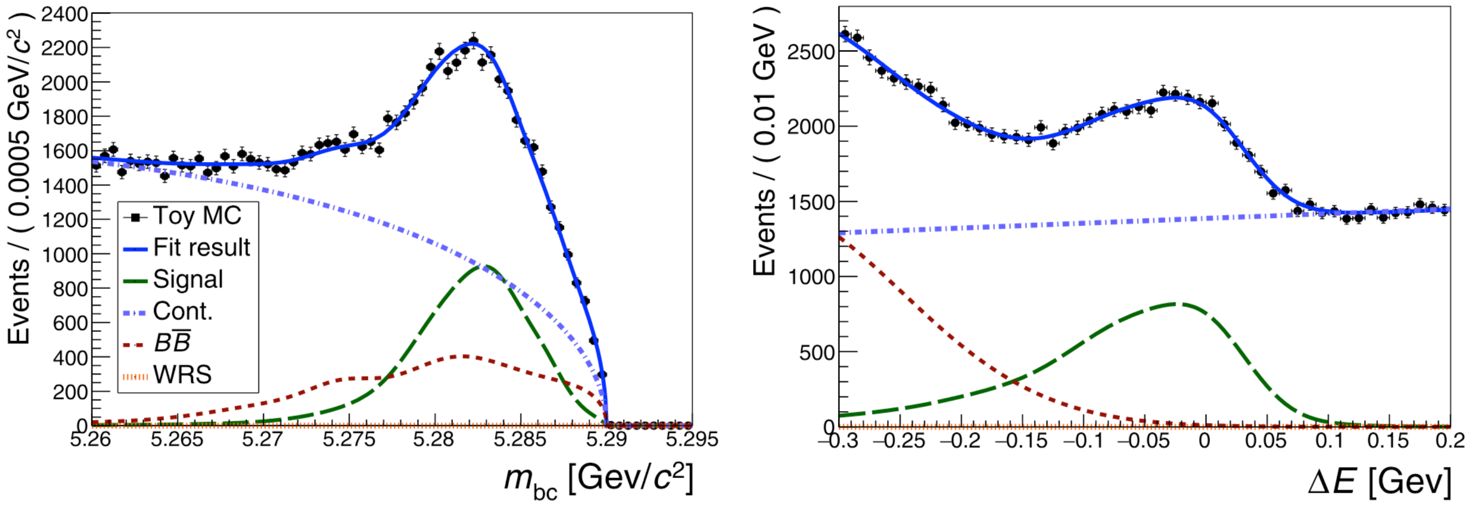

Fig. 113. Projections of the fit results for candidates reconstructed as $B^0 \to \pi^0(\to \gamma\gamma)\,\pi^0(\to \gamma\gamma)$. The projections for one example pseudo-experiment are shown onto $M_{\rm bc}$ (left) and ΔE (right). Points with error bars represent the toy sample. The full fit results are shown by the solid blue curves. Contributions from signal, generic $B\bar{B}$ events, continuum background, and background from wrongly reconstructed signal events are shown by the long dashed green, short dashed red, dash-dotted blue, and dotted orange curves, respectively. The input values used for this pseudo-experiment are $A_{\pi^0\pi^0} = 0.34$ and $S_{\pi^0\pi^0} = 0.65$.

$B\bar{B}$ background Sources of background from $B\bar{B}$ events are studied with a $4\,\text{ab}^{-1}$ MC sample. The largest contribution comes from $B^+ \to \rho^+(\to \pi^+\pi^0)\pi^0$ decays, where the π^+ is lost. Events where the remaining π^0 pair decays into four photons which arrive at the ECL are the main $B\bar{B}$ background for $B^0 \to \pi^0_{\gamma\gamma}\pi^0_{\gamma\gamma}$ candidates. Those events which contain a converted photon or a Dalitz π^0 are the main background $B\bar{B}$ source for $B^0 \to \pi^0_{\rm dal}\pi^0_{\gamma\gamma}$ candidates. This background peaks at the same value of $M_{\rm bc}$, but is shifted in ΔE towards negative values due to the missing π^+.